of the $S_2O_7^{2-}$ ion constituting the solvent melt should be noted.

The IR spectrum of the compound $Na_2VO(SO_4)_2$, isolated previously,[11] shows a close analogy to the spectrum given here (Figure 4). This is also obvious from the frequencies listed in Table IV, which support the impression that we are dealing with the same compound. Apart from this, only a few sulfato compounds of V(IV) have been examined by IR spectroscopy, and so far, no Raman spectra have been published except[7] for that of the compound $K_4(VO)_3(SO_4)_5$. For α- and β-$VOSO_4$ the IR spectra show[12,15,22,23] that the ν(V=O) bands are found in the region 940–990 cm^{-1} while $\nu_1(SO_4^{2-})$ and split $\nu_3(SO_4^{2-})$ bands are present in the region 1000–1200 cm^{-1}. Several bands of the bending modes, $\nu_2(SO_4^{2-})$ and $\nu_4(SO_4^{2-})$, respectively, are found in the regions of ca. 400–500 and ca. 600–700 cm^{-1}. An identical compound, which probably can be represented by the formula $K_2(VO)_2(SO_4)_3$, seems to have been obtained in three different investigations according to the stoichiometry and the IR spectra of the compounds.[12,23,24] In these investigations ν(V=O) bands are found around 985 cm^{-1}, while the ν_1 and ν_3 stretching modes of the SO_4^{2-} groups are found in the region 1000–1270 cm^{-1} and the ν_2 and ν_4 bending modes in the regions ca. 400–460 and 600–660 cm^{-1}, respectively. The complicated IR and Raman spectra[7] of the compound $K_4(VO)_3(SO_4)_5$ show that the stretching modes ν(V=O), $\nu_1(SO_4^{2-})$, and $\nu_3(SO_4^{2-})$ most probably are found in the region 970–1270 cm^{-1} and the bending modes $\nu_4(SO_4^{2-})$ and $\nu_2(SO_4^{2-})$ at 600–700 and 440–520 cm^{-1}, respectively. For $K_2VO(SO_4)_2$, the potassium analogue of the sodium compound studied here, the IR spectrum shows[12] rather similar features, as can be seen in Table IV. The ν(V=O) bands seem to be found at lower frequencies in $Na_2VO(SO_4)_2$ than in $K_2VO(SO_4)_2$. The same is found by comparison to $K_4(VO)_3(SO_4)_5$.[7] This seems reasonable since the V=O bond length is longer in $Na_2VO(SO_4)_2$ than in $K_4(VO)_3(SO_4)_5$. This weakening of the V=O bond in $Na_2VO(SO_4)_2$ might be due to a stronger donation of electrons to the metal d orbitals by the sulfate ligand opposite the V=O bond. This is reflected by the unusual short opposite V—O bond length of 2.15 Å in $Na_2VO(SO_4)_2$ compared to 2.22–2.23 Å found in $K_4(VO)_3(SO_4)_5$. A general common feature for all V(IV) oxo–sulfato compounds discussed here seems to be—judged from the vibrational spectra—the presence of bi- or tridentate chelate or bridging sulfate ligands coordinated to a $V{=}O^{2+}$ entity. The X-ray structure examinations made so far confirm this.

Conclusion

The compound $Na_2VO(SO_4)_2$ has been isolated from the liquid–gas system $V_2O_5/K_2S_2O_7$–$SO_2/O_2/N_2$ and its molecular structure determined. The deactivation of sulfuric acid catalysts at lower temperatures has been attributed[25] to the precipitation of V(IV) compounds. Indeed, our recent work[8] has shown that when V(III) and V(IV) compounds of the alkali metals Na, K, and Cs are formed in the $M_2S_2O_7/V_2O_5$–$SO_2/O_2/N_2$ liquid–gas system (M = Na, K, Cs), a similar dramatic decrease in the catalytic activity of the system is observed. Thus, the precipitation of the V(IV) compound $Na_2VO(SO_4)_2$ may contribute to the observed deactivation at low temperatures of the commercial catalyst containing sodium as a copromotor to potassium.

Acknowledgment. This investigation was in part supported by the Danish Technical Research Council.

Supplementary Material Available: Tables A and C, giving temperature factor parameters and all crystallographic data (2 pages); Table B, listing observed and calculated structure factors (8 pages). Ordering information is given on any current masthead page.

(22) Tudo, J. *Rev. Chim. Miner.* **1965**, *2*, 53.
(23) Ezhkova, Z. I.; Zaitsev, B. E.; Konysheva, L. I.; Matveevicheva, V. A.; Nekhorosheva, N. I.; Polotnyuk, O.-V. Y.; Chaikovskii, S. P. *Kinet. Katal.* **1972**, *13*, 1288; *Kinet. Catal. (Engl. Transl.)* **1972**, *13*, 1149.
(24) Bazarova, Z. G.; Boreskov, G. K.; Ivanov, A. A.; Karakchiev, L. G.; Kacohkina, L. D. *Kinet. Katal.* **1971**, *12*, 948; *Kinet. Catal. (Engl. Transl.)* **1971**, *12*, 845.
(25) Mastikhin, V. M.; Polyakova, G. M.; Zyulkovskii, Y.; Boreskov, G. K. *Kinet. Katal.* **1970**, *11*, 1463; *Kinet. Catal. (Engl. Transl.)* **1970**, *11*, 1219.

Contribution from the Institute of Chemistry Academia Sinica, Nankang, Taipei, Taiwan, Republic of China

$RbV_3P_4O_{17+x}$ (x = 0.14): A Novel Mixed-Valence Vanadium Pyrophosphate

K. H. Lii* and C. S. Lee

Received December 21, 1989

A novel mixed-valence vanadium pyrophosphate, $RbV_3P_4O_{17+x}$ (x = 0.14), was discovered, and its structure was determined from single-crystal X-ray diffraction data. This nonstoichiometric phase crystallizes in the tetragonal space group $P4_2/mnm$ with a = 13.651 (2) Å, c = 7.289 (2) Å, V = 1358.3 (4) Å^3, Z = 4, R = 0.0366, and R_w = 0.0360 for 835 unique reflections with $I > 2.5\sigma(I)$. The structure may be regarded as built from ReO_3-type infinite chains along the c axis (in which each VO_6 octahedron shares two opposite vertices) and finite chains parallel to the ⟨110⟩ directions, which are linked by P_2O_7 groups to form a three-dimensional structure. Each finite chain consists of four VO_6 subunits. The oxygen atom shared between the central and side octahedra in the four-membered chain is about two-thirds occupied. Variable-temperature powder magnetic susceptibility data suggest the presence of two V^{4+} and one V^{5+} per formula unit and support the formula determined from single-crystal X-ray diffraction data.

Introduction

The vanadium phosphorus oxide system has shown a rich structural chemistry owing to the accessibility of more than one oxidation state and the ability of vanadium polyhedra and phosphate tetrahedra to form a variety of frameworks. As a part of the search for novel mixed frameworks built up from corner-sharing octahedra and tetrahedra, we recently began an investigation of the vanadium phosphate system containing vanadium in oxidation states less than +5. By adding alkali-metal cations to this system, a variety of structural types with cage, tunnel, or layer structures have been generated. In the system M–V(IV)–P–O, $LiVOPO_4$,[1] $M_2VOP_2O_7$ (M = K, Rb, Cs),[2,3] and $M_2V_3P_4O_{17}$ (M = Cs, Rb, K)[4-6] are known to exist. The phos-

(1) Lavrov, A. V.; Nikolaev, V. P.; Sadikov, G. G.; Porai-Koshits, M. A. *Sov. Phys.—Dokl. (Engl. Transl.)* **1982**, *27*, 680.
(2) Gorbunova, Yu. E.; Linde, S. A.; Lavrov, A. V.; Tananaev, I. V. *Dokl. Akad. Nauk SSSR* **1980**, *250* (2), 350.
(3) Lii, K. H.; Wang, S. L. *J. Solid State Chem.* **1989**, *82*, 239.
(4) Lii, K. H.; Wang, Y. P.; Wang, S. L. *J. Solid State Chem.* **1989**, *80*, 127.

0020-1669/90/1329-3298$02.50/0

phates of V(III) include $Cs_3V_3P_{12}O_{36}$,[7] $CsV_2P_3O_{16}$,[8] $Na_3V_2P_3O_{12}$,[9] and MVP_2O_7 (M = Li, Na, K, Rb, Cs).[10-12] Recently, an interesting mixed-valence vanadium phosphate containing V(II) and V(III), $NaV_3P_3O_{12}$,[13] was reported. Mixed-valence compounds have been the subject of innumerable studies because of their interesting physical properties. To our knowledge, mixed-valence vanadium phosphates have been rare. We thus initiated a synthetic program to explore novel mixed-valence compounds in the system of alkali-metal vanadium phosphates. The present paper deals with the preparation, crystal structure, and magnetic susceptibility of the mixed-valence vanadium pyrophosphate $RbV_3P_4O_{17+x}$ (x = 0.14).

Experimental Section

Synthesis. $Rb_4V_2O_7$ (99.9%), V_2O_5 (99.9%), and P_2O_5 (99.9%), obtained from Cerac Inc., were used as received. Loading of the reactants was carried out in a glovebox that was flushed with nitrogen. The title compound was first obtained as dark green crystals in an attempt to prepare "$RbV_2P_3O_{13}$" by heating a pressed pellet of $Rb_4V_2O_7$, V_2O_5, and P_2O_5 (mole ratio 1:3:6) in a sealed silica tube at 700 °C for 48 h followed by slow cooling to room temperature. It gave a sharp report when the silica ampul was opened with a hammer. The pressure in the ampul was due to the loss of oxygen, as is known to occur for V^{5+} compounds. A single-crystal X-ray diffraction study showed the crystal to be the new compound $RbV_3P_4O_{17+x}$ (x = 0.14). Subsequently, this air-stable nonstoichiometric phase was prepared in nearly pure form by reaction of $Rb_4V_2O_7$, V_2O_5, and P_2O_5 in a mole ratio of 1:5:8 at 650 °C for 2 days in a sealed silica tube and then at 700 °C for 2 days in air with intermediate grinding. The reason the starting materials were first heated in a sealed container was to prevent the loss of volatile P_2O_5. X-ray powder diffraction patterns for identification purposes were obtained by using a Rigaku powder diffractometer with filtered copper radiation. On the basis of X-ray analysis, the dark green polycrystalline products were always contaminated with very small amounts of unidentified impurities. The intensity of the most intense reflection of the impurities was about 4% that of the major phase, and all other reflections in the diffraction pattern corresponded well with that calculated from the single-crystal data. The compound appeared air-stable in the laboratory atmosphere for at least several hours and was checked by powder X-ray diffraction and infrared spectroscopy. An IR spectrum in the 3000–4000-cm^{-1} range did not reveal the presence of OH groups. A differential thermal analysis performed in air showed that the material melted with decomposition at 820 °C. A powder X-ray diffraction analysis indicated that the decomposition product was amorphous.

Magnetic Measurements. Variable-temperature magnetic susceptibility $\chi(T)$ data were obtained on 253.88 mg of polycrystalline sample from 4 to 300 K in a magnetic field of 3 kG by using a Quantum Design SQUID magnetometer. Diamagnetic contributions for Rb^+, V^{5+}, and P^{5+} were estimated as suggested by Selwood,[14] and that for O^{2-} was estimated as suggested by Sienko et al.[15] for a solid-state network. These were subtracted from the experimental susceptibility data to obtain the molar paramagnetic susceptibilities of the compound. The data were least-squares-fitted from 4 to 300 K to the relation $\chi_M = C/(T - \Theta)$, where C is the molar Curie constant and Θ is the Weiss constant.

Single-Crystal X-ray Diffraction. A dark green crystal having the dimensions 0.2 × 0.2 × 0.15 mm was selected for indexing and intensity data collection on an Enraf Nonius CAD4 diffractometer with graphite-monochromated Mo Kα radiation. The orientation matrix and unit cell parameters were determined at room temperature by a least-squares fit of 25 peak maxima with $19° < 2\theta < 27°$. Axial oscillation photographs along the three axes were taken to check the symmetry properties and unit cell parameters. Of the 2110 reflections measured (maximum $2\theta = 60°$, octants collected $+h,+k,+l$, scan mode $\omega - 2\theta$), 1113 were unique and 835 reflections were considered observed ($I > 2.5\sigma(I)$) after Lp and empirical absorption corrections. Corrections for absorption effects were based on ψ scans of a few suitable reflections with χ values close to 90°.[16] An examination of the intensity data showed $4/mmm$ Laue symmetry and the systematic absences $k + l = 2n + 1$ for $0kl$ reflections, $h = 2n + 1$ for $h00$ reflections, and $l = 2n + 1$ for $00l$ reflections. On the basis of statistical distribution and successful solution and refinement of the structure, the space group was determined to be $P4_2/mnm$ (No. 136). Direct methods (NRCVAX)[17] were used to locate the metal atoms, and the phosphorus and oxygen atoms were located by using the Fourier synthesis section of the program. In the last stage of least-squares refinement, SHELXTL-PLUS programs[18] were used. Neutral-atom scattering factors and corrections for anomalous dispersion were from common sources.[19]

Atoms V(2) and V(3), which were located at 4g special positions, exhibited very large U_{11} and U_{22} values. A difference Fourier map showed large residual electron densities near both the V(2) and V(3) positions, which could be interpreted as disorder between two sites. Therefore, a model of two disordered sites for atoms V(2) and V(3) was used with constraints applied to their occupancy factors and thermal parameters. The thermal parameters for two disordered vanadium sites were constrained to be the same, and the sum of their occupancy factors

Table I. Crystallographic Data for $RbV_3P_4O_{17+x}$ (x = 0.14)

$RbV_3P_4O_{17.14}$	T = 23 °C
space group = $P4_2/mnm$ (No. 136)	λ = 0.709 30 Å
fw = 636.413	ρ_{calcd} = 3.112 g cm^{-3}
a = 13.651 (2) Å	μ = 59.9 cm^{-1}
c = 7.289 (4) Å	transm coeff = 0.804–0.999
V = 1358.3 (4) Å^3	$R(F_o)$ = 0.0366
Z = 4	$R_w(F_o)$ = 0.0360

Table II. Atomic Coordinates and Equivalent Isotropic Thermal Parameters (×10^2) for $RbV_3P_4O_{17+x}$ (x = 0.14)

atom	x	y	z	occ	U_{eq}, Å^2[a]
Rb	0.19973 (6)	0.19973 (6)	0.0	1.0	3.45 (3)
V(1)	0.5	0.0	0.25	1.0	3.13 (6)
V(2)	0.6612 (1)	0.6612 (1)	0.5	0.876 (2)	0.82 (4)
V(2)′	0.3076 (8)	0.3076 (8)	0.5	0.124 (2)	0.82 (4)
V(3)	0.1281 (1)	0.1281 (1)	0.5	0.536 (1)	0.77 (4)
V(3)′	0.0815 (2)	0.0815 (2)	0.5	0.464 (1)	0.77 (4)
P(1)	0.47399 (7)	0.23352 (7)	0.8016 (1)	1.0	0.77 (2)
O(1)	0.0	0.0	0.5	1.0	2.2 (2)
O(2)	0.5	0.0	0.0	1.0	1.8 (2)
O(3)	0.1786 (2)	0.0412 (2)	0.6906 (4)	1.0	1.24 (8)
O(4)	0.5276 (2)	0.1424 (2)	0.7502 (4)	1.0	1.29 (8)
O(5)	0.2518 (2)	0.3849 (2)	0.6812 (4)	1.0	1.56 (8)
O(6)	0.4248 (3)	0.2204 (3)	0.0	1.0	1.2 (1)
O(7)	0.9186 (4)	0.0814 (4)	0.0	1.0	2.6 (2)
O(8)	0.2116 (5)	0.2116 (5)	0.5	0.64 (1)	1.8 (2)

[a] Equivalent isotropic U is defined as one-third of the trace of the orthogonalized U_{ij} tensor.

Table III. Bond Distances (Å) for $RbV_3P_4O_{17+x}$ (x = 0.14)

Rb(1)–O(3)	3.139 (3) (4×)[a]	Rb(1)–O(6)	3.086 (4) (2×)
V(1)–O(2)	1.822 (0) (2×)	V(1)–O(4)	1.980 (3) (4×)
V(2)–O(5)	1.884 (3) (4×)	V(2)–O(7)	1.542 (2)
V(2)–O(8)	2.455 (10)	V(2)–V(2)′	0.600 (16)
V(2)′–O(5)	1.854 (4) (4×)	V(2)′–O(7)	2.142 (15)
V(2)′–O(8)	1.855 (18)	V(3)–O(1)	2.473 (3)
V(3)–O(3)	1.953 (3) (4×)	V(3)–O(8)	1.612 (10)
V(3)–V(3)′	0.900 (4)	V(3)′–O(1)	1.573 (3)
V(3)′–O(3)	1.998 (3) (4×)	V(3)′–O(8)	2.512 (10)
P(1)–O(3)	1.511 (3)	P(1)–O(4)	1.491 (3)
P(1)–O(5)	1.521 (3)	P(1)–O(6)	1.604 (2)

[a] Number of times the distance occurs per formula unit.

(5) Lii, K. H.; Wang, Y. P.; Cheng, C. Y.; Wang, S. L.; Ku, H. C. *J. Chin. Chem. Soc. (Taipei)* **1990**, *37*, 141.
(6) Leclaire, A.; Chahboun, H.; Groult, D.; Raveau, B. *J. Solid State Chem.* **1988**, *77*, 170.
(7) Lovrov, A. V.; Nikolaev, V. P.; Sadikov, G. G.; Voitenkov, M. Ya. *Sov. Phys.—Dokl. (Engl. Transl.)* **1981**, *26*, 631.
(8) Klinkert, B.; Jansen, M. *Z. Anorg. Allg. Chem.* **1988**, *567*, 87.
(9) Delmas, C.; Olazcuaga, R.; Cherkaoui, F.; Brochu, R.; Le Flem, G. *C. R. Seances Acad. Sci., Ser. C* **1978**, *287* (5), 169.
(10) Lii, K. H.; Wang, Y. P.; Chen, Y. B.; Wang, S. L. *J. Solid State Chem.* **1990**, *86*, 143.
(11) Wang, Y. P.; Lii, K. H.; Wang, S. L. *Acta Crystallogr.* **1989**, *C45*, 673.
(12) Wang, Y. P.; Lii, K. H. *Acta Crystallogr.* **1989**, *C45*, 1210.
(13) Kinomura, N.; Matsui, N.; Kumada, N.; Muto, F. *J. Solid State Chem.* **1989**, *79*, 232.
(14) Selwood, P. W. *Magnetochemistry*; Interscience: New York, 1956.
(15) Sienko, M. J.; Banerjee, B. *J. Am. Chem. Soc.* **1961**, *83*, 4149.
(16) Alcock, N. W. *Acta Crystallogr.* **1974**, *A30*, 332.
(17) Larson, A. C.; Lee, F. L.; Le Page, Y.; Gabe, E. J. *The NRC VAX Crystal Structure System*; National Research Council of Canada: Ottawa, Canada, 1986.
(18) Sheldrick, G. M. *SHELXTL-PLUS Crystallographic System, Version 2*; Nicolet XRD Corp.: Madison, WI, 1986.
(19) Cromer, D. T.; Weber, J. T. *International Tables for X-Ray Crystallography*; Kynoch Press: Birmingham, England, 1974; Vol. IV.

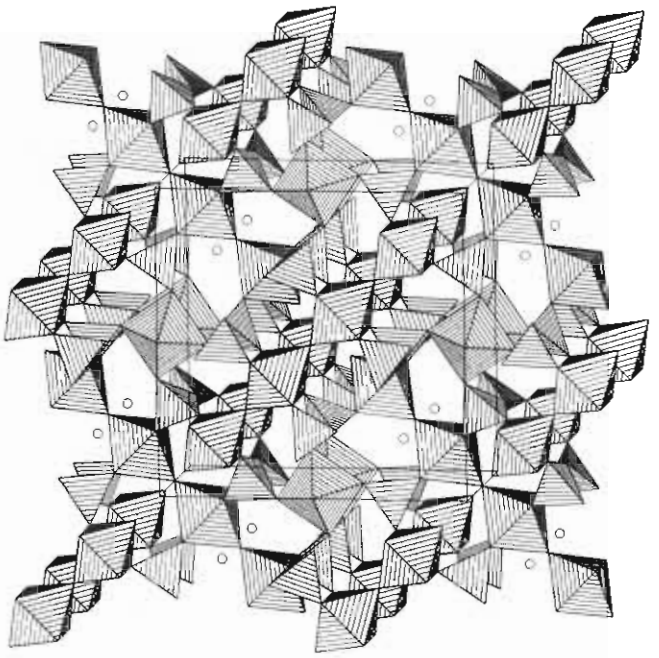

Figure 1. Polyhedron representation displaying the framework of $RbV_3P_4O_{17+x}$ ($x = 0.14$) in a direction approximately parallel to the c axis. In this representation, the corners of octahedra and tetrahedra are O^{2-} ions, the V and P ions are at the center of each octahedron and tetrahedron, respectively, and the circles represent Rb^+ ions.

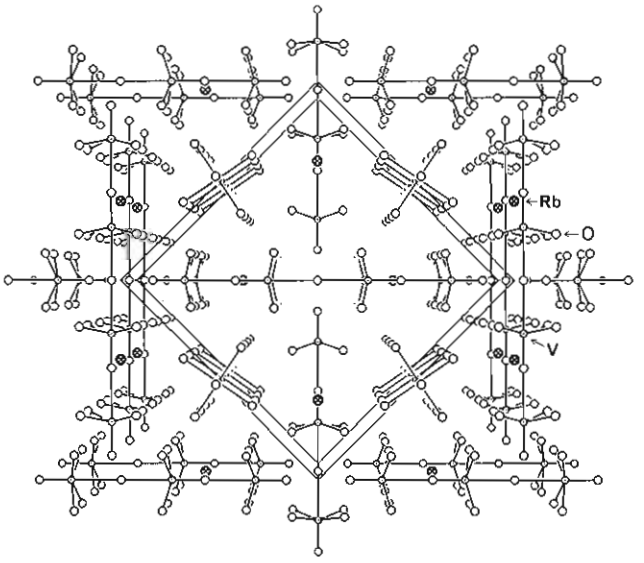

Figure 2. Perspective view of the structure along the c axis. For clarity, the P_2O_7 groups and V ions at the V(2)′ and V(3)′ sites are not shown.

was set equal to 1. Actually atom V(1) also exhibited a large U_{33} thermal parameter, suggesting positional disorder along the c axis. However, a model including disordered V(1) was unsuccessful. Isotropic refinement of atoms V(2) and V(3) and anisotropic refinement of all other atoms gave final residuals of $R = 0.040$ and $R_w = 0.042$. At this stage of refinement, it was noted that atom O(8) had a large U_{eq} of 0.060 (3) Å^2. The occupancy factor of each atom was then allowed to refine, but only that for O(8) deviated significantly from full occupancy. The O(8) position refined to an occupancy of 0.64 (1), which led to the refined composition $RbV_3P_4O_{17+x}$ ($x = 0.14$). The final cycle of full-matrix least-squares refinement gave R and R_w values of 0.0366 and 0.0360, respectively. A few $\sim\pm1.8$ e/Å^3 residuals were located near the vanadium sites, which could be due to the incomplete modeling of the disordered vanadium atoms. The final difference map at other atom sites was flat to less than ±1 e/Å^3.

Results and Discussion

Structure. Table I lists the crystallographic data. Final atomic coordinates and equivalent isotropic thermal parameters (U_{eq}) are

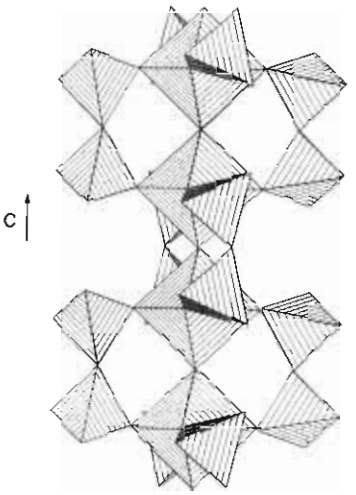

Figure 3. Section of a $[V_2P_8O_{30}]_\infty$ chain in $RbV_3P_4O_{17+x}$ ($x = 0.14$).

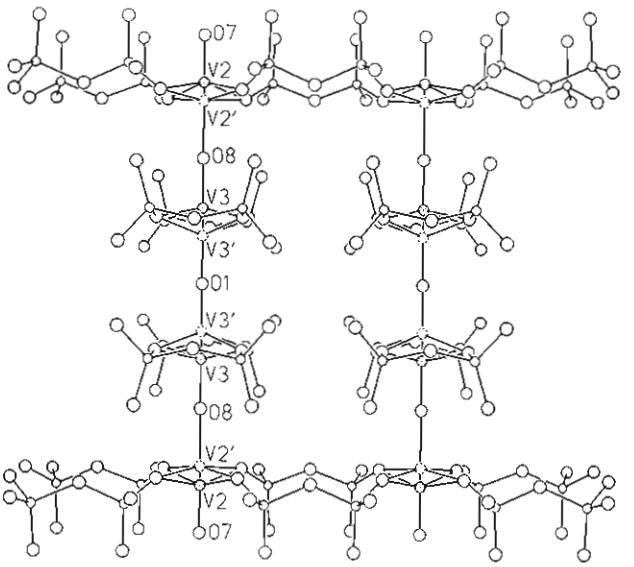

Figure 4. Two adjacent four-membered chains in $RbV_3P_4O_{17+x}$ ($x = 0.14$).

listed in Table II. Selected interatomic distances are given in Table III. A polyhedron representation (STRUPLO84[20]) in a direction approximately parallel to the c axis is presented in Figure 1. A perspective view of the structure is shown in Figure 2, in which P_2O_7 groups and the V ions at the V(2)′ and V(3)′ sites are omitted for clarity. Although the composition of the title compound appears somewhat related to that of $M_2V_3P_4O_{17}$ (M = Cs, Rb, K),[4-6] its structure is markedly different. The framework of $RbV_3P_4O_{17+x}$ ($x = 0.14$) is built of infinite chains along the c axis and finite chains parallel to the ⟨110⟩ directions, which are linked together in three dimensions by P_2O_7 groups. Both types of chains are formed of trans-corner-sharing VO_6 octahedra. The infinite chain is composed of $V(1)O_6$ octahedra, and each pyrophosphate group forms a bridge over two adjacent octahedra within a chain, forming $[V_2P_8O_{30}]_\infty$ along the c axis (Figure 3). The finite chain consists of four VO_6 subunits (Figure 4). Each central octahedron, $V(3)O_6$, is chelated by two P_2O_7 groups, and each side octahedron, $V(2)O_6$, shares four monodentate P_2O_7 groups with two adjacent finite chains. Each P_2O_7 group shares its six vertices with one infinite chain and three finite chains.

Atom V(1) shows large U_{33} value indicative of positional disorder along the c axis. The vanadium atoms within the infinite chain may actually be arranged with alternately short and long V(1)–O(2) distances. Infinite V=O···V=O···V=O chains have

(20) Fischer, R. X. *J. Appl. Crystallogr.* **1985**, *18*, 258.

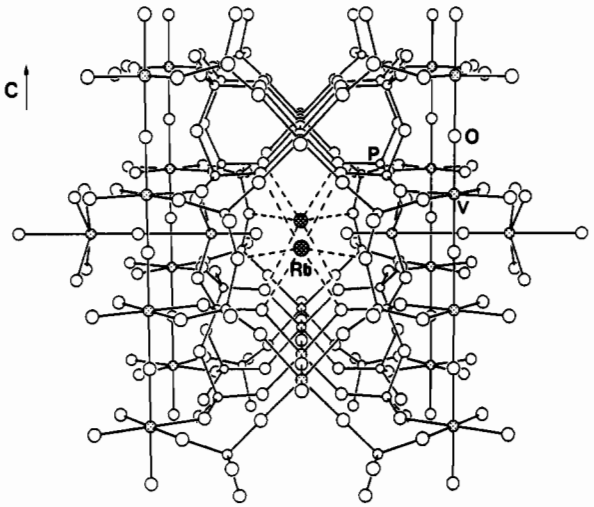

Figure 5. View of the coordination environment of Rb^+ in $RbV_3P_4O_{17+x}$ (x = 0.14) in [110] direction.

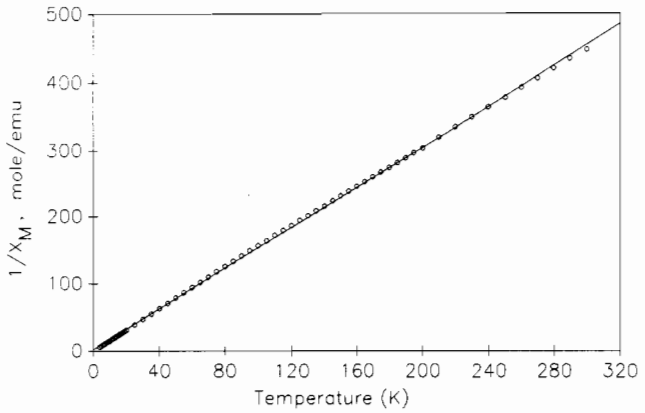

Figure 6. Inverse molar magnetic susceptibility as a function of temperature for $RbV_3P_4O_{17+x}$ (x = 0.14). The solid line represents a least-squares fit to the data from 4 to 300 K according to $\chi = C/(T - \Theta)$.

also been observed in α-VPO_5[21] and VP_2SiO_9.[22] Atoms V(2) and V(3) in the four-membered chain are also disordered. Atom V(2) is disordered in two sites with one site predominant. In contrast, atom V(3) is disordered in two sites with one site slightly preferable to the other. The O(8) site, which is the intrachain link between the central and side VO_6 octahedra of the finite chain, has a refined occupancy of 0.64 (1), giving a phase composition of $RbV_3P_4O_{17+x}$ (x = 0.14). If the O(8) site is half-occupied, then the composition becomes $RbV_3P_4O_{17}$. An empty O(8) site would result in an unlikely configuration of two $V(3)O_5$ square pyramids sharing the axial oxygen, O(1), which has not been reported in vanadium phosphates. Vanadium ions at V(2), V(3), and V(3)′ sites have a common environment, which is a gross distortion of octahedron; one short V–O bond length is 1.54–1.61 Å, which is about 0.4 Å shorter than the four equatorial V–O bonds, but the sixth bond is much longer, ~2.5 Å, and the coordination is better regarded as distorted square pyramidal. The geometry is "distorted" in the sense that the vanadium atom lies above the plane of the four basal oxide ligands. This geometry often occurs with compounds containing the oxovanadium(IV) ion or oxovanadium(V) ion. The less important V(2)′ site has a distorted octahedral environment with one axial and four equatorial oxygens at 1.85 Å and an axial V–O bond of 2.14 Å. It should be noted that the equatorial V–O bonds for atom V(2) are significantly shorter than the corresponding bond lengths for other V atoms, indicative of higher valence for atom V(2). The average valence of V in $RbV_3P_4O_{17+x}$ (x = 0.14) is +4.43 and suggests that V^{5+} and V^{4+} are simultaneously present in the structure. Of most interest is the charge distribution among different V ions. The valence of V can be assessed by summing the bond valences of V–O bonds. Using the Brown–Altermatt form for the bond length–bond valence relation,[23] bond valence = $e^{(R-d_{V\text{-}O})/0.37\text{Å}}$, where R = 1.784 Å for V^{4+}–O, we obtain the following results: V(1), +4.16; V(2), +5.09; V(2)′, +4.51; V(3), +4.28; V(3)′, +4.15. The summation of the assessed valences, assuming +5 for V(2) and taking into account the occupancy factors, is equal to 13.32, which is in good agreement with the value of +13.28 based on the stoichiometry. This encouraging result suggests that the valence for atom V(2) is +5 and those for atoms V(1) and V(3) are mostly +4. However, it is not obvious that V ions at V(1), V(3), and V(3)′ sites are preferably reduced to V^{4+}. Bond strength sums about the oxygen atoms are as follows: O(2), 1.80; O(8), 1.76; O(6), 2.18; other oxygen atoms, 1.92–2.06. The somewhat lower values for O(2) and O(8) could be attributed to the disordered vanadium atoms. Atom O(6), the bridging atom of the pyrophosphate group, has a somewhat higher bond strength sum, which often occurs for the bridging oxygen atoms of vanadium(IV) pyrophosphates.

The PO_4 tetrahedra forming the pyrophosphate group exhibit an eclipsed configuration, since the bridging oxygen atom, O(6), resides on a mirror plane. The P atoms are displaced away from O(6), giving rise to three shorter and one longer P–O bonds. The P–O(6)–P bond angle is 128.7 (3)°. Figure 5 shows the coordination environment for the Rb^+ cations. Each Rb^+ cation is located in a cage surrounded by two infinite and two finite chains. The coordination number of Rb^+ can be determined by the maximum bond distance for Rb–O by using the procedure of Donnay and Allmann[24] with the revised radii of Shannon,[25] leading to 3.42 Å. Accordingly, Rb^+ is coordinated by two O(6) and four O(3) atoms at distances of 3.086 (4) and 3.139 (3) Å, respectively. The Rb^+ cation is loosely bonded to the oxygen atoms, and it has a bond valence sum of 0.59, which is much lower than the expected value of 1.0. The cages appear too large for Rb^+ cations, which is also indicated by the high thermal parameter of Rb.

Magnetic Susceptibility. Figure 6 shows a plot of the reciprocal molar susceptibility for $RbV_3P_4O_{17+x}$ (x = 0.14) as a function of temperature. No evidence for magnetic ordering was observed down to 4 K, suggestive of independent paramagnetic spins of V ions in the structure. The solid line in the figure is the fit according to $\chi = C/(T - \Theta)$ with the Curie constant C = 0.663 cm^3 K/mol and the Weiss constant Θ = −1.61 K. From the relation $C = N\mu_{eff}^2/3k_B$, one obtains the effective magnetic moment μ_{eff} = 2.30 μ_B per formula unit, which is close to theoretical value, 2.40 μ_B, for two independent spins of V^{4+} per formula unit. The theoretical value for the effective moment of V^{4+} ($3d^1$), assuming complete quenching of the orbital angular momentum, is given by $g[S(S + 1)]^{1/2}$ = 1.70 μ_B, where $S = {}^1/_2$ and g, determined from ESR studies, is 1.963. The results of this magnetic study are consistent with the stoichiometry $RbV_3P_4O_{17}$ (1 V^{5+}, 2 V^{4+}) and provide strong evidence for the elimination of the formula $RbV_3P_4O_{17.5}$ (2 V^{5+}, 1 V^{4+}). However, the magnetic susceptibility data may not be able to distinguish the difference between $RbV_3P_4O_{17}$ and $RbV_3P_4O_{17+x}$ (x = 0.14). It should be noted that the single crystal used for structural analysis was grown at 700 °C under an oxygen pressure of approximately 7.5 atm in a sealed silica ampul. The single crystal might have a slightly higher oxygen content than that of the air-sintered powder sample.

Acknowledgment. Support for this study by the National Science Council and the Institute of Chemistry Academia Sinica is gratefully acknowledged. We thank Mr. Y. S. Wen for collecting single-crystal X-ray diffraction data.

Supplementary Material Available: Full listings of crystallographic data (Table S1) and anisotropic thermal parameters (Table S2) (2 pages); a listing of the observed and calculated structure factors (Table S3) (4 pages). Ordering information is given on any current masthead page.

(21) Jordan, B.; Calvo, C. *Can. J. Chem.* **1973**, *51*, 2621.
(22) Rice, C. E.; Robinson, W. R.; Tofield, B. C. *Inorg. Chem.* **1976**, *15*, 345.
(23) Brown, I. D.; Altermatt, D. *Acta Crystallogr.* **1985**, *B41*, 244.
(24) Donnay, G.; Allmann, R. *Am. Mineral.* **1970**, *55*, 1003.
(25) Shannon, R. D. *Acta Crystallogr.* **1976**, *A32*, 751.